Chemistry and kinetics of the GaN formation by plasma nitridation of GaAs: An *in situ* real-time ellipsometric study

M. Losurdo, P. Capezzuto, and G. Bruno*

Plasma Chemistry Research Center, MITER-CNR, via Orabona, 4 70126 Bari, Italy

E. A. Irene

Department of Chemistry, University of North Carolina, Chapel Hill, North Carolina 27599-3290

The chemistry and kinetics of the nitridation of GaAs (100) surfaces by N_2, N_2-H_2, and N_2-NH_3 radio-frequency plasmas, in a remote configuration, are investigated *in situ* and in real time using spectroscopic ellipsometry. The effects of the surface temperature in the range 70–700 °C and of the gas-phase chemistry on both the nitridation kinetics and the composition of the resulting GaN layer are highlighted. Pure N_2 plasmas yield stoichiometric and smooth GaN layers with As segregation at the GaN/GaAs interface. The As segregation inhibits GaAs nitridation, because the N atoms scavenge the free As, and thereby limits the GaN thickness to a few angstroms. Thicker GaN layers (>100 Å) are obtained by N_2-H_2 and N_2-NH_3 plasmas, since hydrogen reduces the As segregation by the formation and desorption of AsH_x species. For the three plasma mixtures, the self-limiting nature of the GaAs nitridation process is revealed and explained using simple kinetic and chemical models based on the fact that the GaAs nitridation can be considered to be a *topochemical* reaction. Also demonstrated is the ineffectiveness of the nitridation at $T \geqslant 600$ °C, which is accompanied by the GaAs substrate decomposition and yields both a rough and Ga-rich GaN layer. [S0163-1829(98)01247-8]

I. INTRODUCTION

The renaissance in the III-V semiconductor field in the last few years is in large part due to the reports of the first blue light-emitting diodes LED's from Nakamura and co-workers.[1,2] However, despite this technological success that has led to the manufacture of blue lasers based on GaN,[3] relatively little is known about the underlying mechanistic chemistry of the processes involved in the epitaxial growth of GaN films, especially in the initial growth stage. This situation can be summarized by a statement attributed to Pearton and Kuo:[4] ''devices appeared and now people are trying to understand why they actually work.'' It is to this latter objective that the present study of the growth of GaN films is aimed.

One main difficulty encountered in growing GaN-based structures on GaAs substrates is the control of the structural and chemical quality of the epitaxial GaN/GaAs substrate interface, because of the large lattice mismatch of 20% between GaN and GaAs. Surface nitridation of the GaAs substrate[5–9] prior to epitaxial growth has been found to have a crucial influence on the crystalline quality of the final GaN epilayers.[10–13] With respect to this, a variety of results have been reported on the effectiveness of the GaAs substrate nitridation pretreatment for the subsequent GaN epigrowth. As an example, GaAs nitridation can result in layers of cubic GaN (β-GaN), hexagonal GaN (α-GaN) or a mixture of both phases depending on the nitridation process (thermal or plasma-activated),[9,11,12,14] on the nitrogen source (N_2, NH_3, hydrazine, and dimethylhydrazine),[10,11,15] on the nitridation time,[11] and also on the presence of an arsenic stabilizing flux.[16] Moreover, Brandt and co-workers[17,18] reported that the surface stoichiometry can be a crucial parameter controlling the phase purity and, hence, the GaN growth kinetics

and morphology. Thus, the study of the nitridation chemistry and kinetics assumes a noticeable importance and, in particular, questions arise about the fate of the As coming from the anion exchange reaction of GaAs in an N atom environment. Here, it is important to underline that As atom diffusion has a dominant role in {111} planes facetting.[15] In order to address these issues *in situ*, noninvasive, real-time monitoring and characterization of surfaces undergoing nitridation using ellipsometry are herein performed.

This paper focuses on the chemistry and kinetics of the nitridation processes involving (100) GaAs surfaces exposed to the downstream flow of N_2, N_2-H_2, and N_2-NH_3 radio-frequency (rf) plasmas. Remote plasma sources of N atoms are receiving keen attention for the growth and processing of GaN-based materials, since with the use of plasma processing low process temperatures with minimal surface damage can be achieved. The key feature of our approach is to use *in situ* real-time single-wavelength ellipsometry for the kinetic investigation of the nitridation process and spectroscopic ellipsometry (SE) for the study of surface morphology and GaN layer chemistry. In addition, optical emission spectroscopy (OES) and mass spectrometry (MS) are used to fingerprint the gas-phase chemistry; and *ex situ* x-ray photoelectron spectroscopy (XPS) is used to analyze the chemical composition of the GaN layers.

II. EXPERIMENT

GaAs (100) substrates were nitrided in a remote rf plasma metal-organic chemical-vapor deposition system described in detail in Ref. 19.

A preliminary H_2 plasma cleaning was performed at a sample temperature $T = 230$ °C under a H atom flux of about

10^{20} atoms/cm^2 sec for a complete oxide and contamination removal. This is an important step, because it has been demonstrated in a previous study[20] that oxygen acts as a barrier for the GaAs nitridation. Cleaning was immediately followed by GaAs nitridation experiments, which are grouped as follows.

Nitridation performed using N$_2$ plasmas at a rf power of 200 W, N$_2$ fluxes of 100 and 1000 SCCM (SCCM denotes cubic centimeter per minute at STP), corresponding to pressures of 0.2 and 1 Torr, respectively, and at a surface temperature in the range 70–600 °C.

Nitridation performed using N$_2$-H$_2$ plasmas at a rf power of 200 W, a H$_2$/N$_2$ flux ratio of 3/100, a pressure of 0.2 Torr and at a temperature in the range 250–700 °C, a set of experiments was also performed at a pressure of 1 Torr, a N$_2$ flux of 1000 SCCM with a H$_2$/N$_2$ flux ratio in the range 0.002–0.03.

Nitridation performed using N$_2$-NH$_3$ plasmas at a rf power of 200 W, a pressure of 0.2 Torr, a temperature of 250 °C and by varying the NH$_3$/N$_2$ flux ratio in the range 0.03–0.5.

The SE measurements were performed with an *in situ* ellipsometer (UVISEL-ISA, Jobin Yvon), at an incident angle of 70.45° over the 1.5–5.5 eV energy range. SE spectra of the pseudodielectric function $\langle\varepsilon\rangle = \langle\varepsilon_1\rangle + i\langle\varepsilon_2\rangle$ were modeled using the Bruggeman effective medium approximation (BEMA).[21] The data of Aspnes and Studna were used for the pseudodielectric function of c-GaAs (Ref. 22) and a-As.[23] For GaN the uncertainty of the GaN layer crystallinity pushed us to compare the different pseudodielectric functions for the cubic GaN (Ref. 24) and for the hexagonal GaN.[25,26] The pseudodielectric function of free gallium Ga^0 was experimentally measured by preparing a 3-μm-thick metallic Ga film on a glass substrate. Once calculated, the BEMA results were compared with the experimental SE spectra and an unbiased estimator χ^2 (defined in Ref. 27), was used to evaluate the goodness of the fit from which the film layer thickness and constituent volume fractions were derived. The lower the χ^2 value, the better the fit. Real-time single wavelength ellipsometry performed at 4.5 eV, i.e., the photon energy of the GaAs E_2 interband critical point,[28] which is extremely sensitive to surface modifications, was used to monitor the nitridation kinetics.

XPS analysis was performed *ex situ* to characterize the chemical composition of GaN layers and to validate the SE models. A Perkin-Elmer 5300 spectrometer using a Mg $K\alpha$ source at 1253.6 eV was used to acquire spectra of the N $1s$, GA $3d$, and As $3d$ photoelectron peaks. Mixed Gaussian-Lorentzian curves were fit to the spectra, in order to obtain information on the Ga, N, and As bonding configuration.

In order to analyze the gas phase surrounding the substrate surface, optical-emission spectroscopy was used in conjunction with mass spectrometry. The OES data were obtained by using an optical fiber that is connected to a 1024 optical spectrometric multichannel analyzer (OMA), (OMA III from EG&G Princeton Applied Research). The MS data were collected by a Elite-600 quadrupole mass spectrometer from VG-Ges Analysis, sampling with a 100 μm orifice just near the GaAs surface.
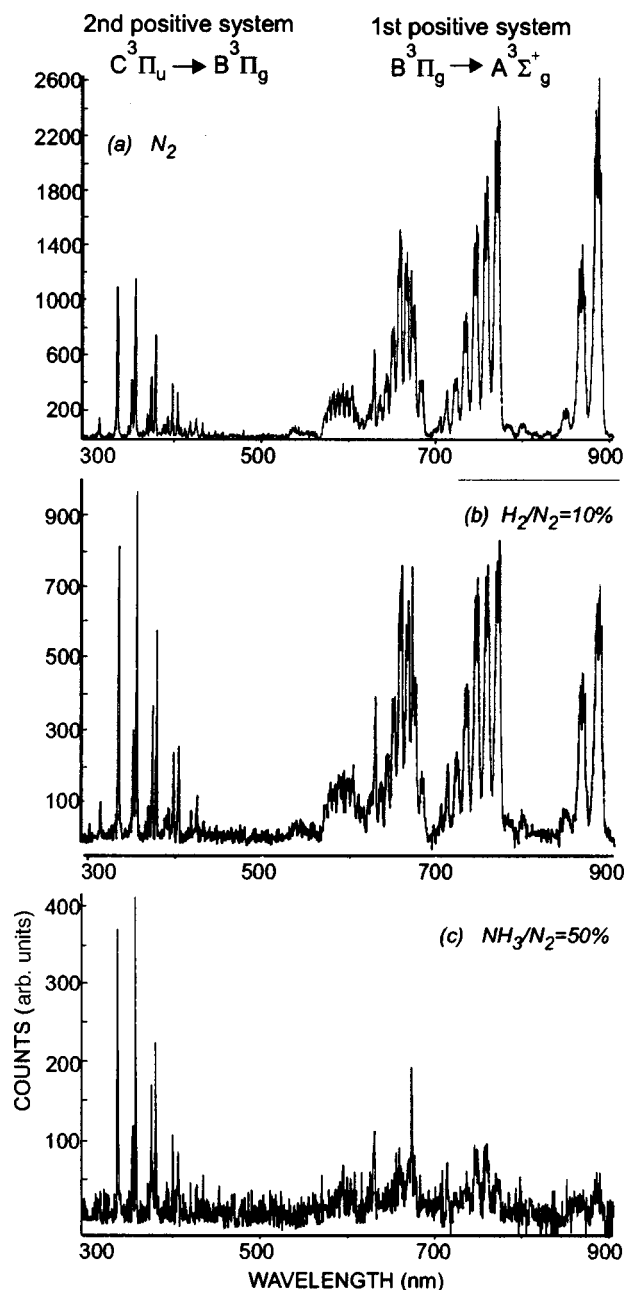
FIG. 1. Typical OES spectra recorded in the afterglow region of (a) N$_2$ plasmas, (b) H$_2$/N$_2$=10/100 plasmas, and (c) NH$_3$/N$_2$=50/50 plasmas at a rf power of 200 W and a pressure of 0.2 Torr.

III. RESULTS AND DISCUSSION

A. OES and MS analysis of the gas phase

Combined MS and OES analyses have been performed to fingerprint the gas-phase environment at the GaAs surfaces during nitridation.

Typical-emission spectra recorded for N$_2$, N$_2$-H$_2$, and N$_2$-NH$_3$ plasmas are shown in Fig. 1. In the spectra dominant are the emission peaks from the N$_2$ in the ranges[29] 500–800 nm and 300–450 nm due, respectively, to the following radiative decay processes:

$$N_2(B^3\Pi_{g}) \rightarrow N_2(A^3\Sigma_u^+) + h\upsilon \text{ (first positive system)},$$

$$(1)$$
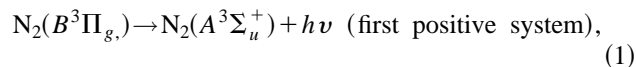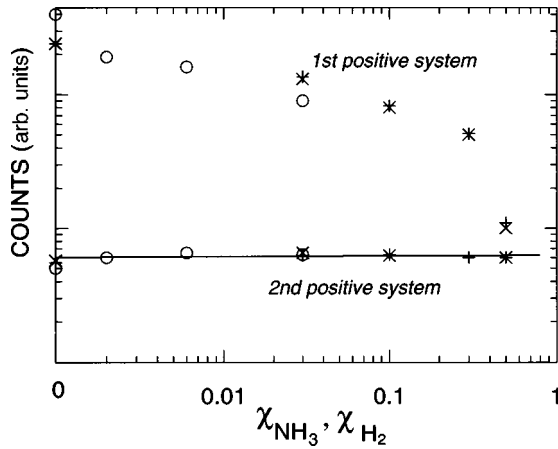
FIG. 2. Normalized emission intensities of the lines at 762.6 and 388.2 nm of the N_2 first and second positive system, respectively, vs the addition of H_2 to N_2 plasmas operated at ($\bigcirc$) 1 Torr and at ($\times$) 0.2 Torr, and ($+$) the addition of NH_3 to N_2 plasmas at 0.2 Torr.

$$N_2(C^3\Pi_{u,}) \rightarrow N_2(B^3\Pi_g) + h\nu \quad \text{(second positive system)}. \tag{2}$$
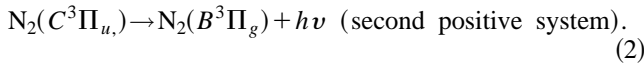
The $N_2{}^+$ first negative emission at 391.4 nm has only been detected in the active-plasma region, and is completely absent in spectra recorded by observing the plasma afterglow near the GaAs surface. Also, emission lines of excited nitrogen atoms by direct electron impact excitation of N atoms, are absent in the spectra. These last observations indicate that electrons are absent at the substrate position where the OES sampling is performed. Thus, under our experimental conditions, the GaAs surface is really in the plasma afterglow region, and any effect of ions and/or energetic electrons on the nitridation kinetics must be excluded.

Figure 2 shows the effect of total pressure and of H_2 and/or NH_3 addition to N_2 plasmas on the N_2 first and second positive emission systems. A decrease of the first positive system emission intensity with an increase of the H_2 and/or NH_3 percentage is observed, whereas the intensity of the second positive system is unaffected. The constant intensity of the second positive system and the experimental observation that, in the OES spectra, the vibrational distribution of the first and second positive systems do not significantly change with H_2 and/or NH_3 dilution indicate that the emission intensities are not affected by the variation of the electron-energy distribution function and of the N_2 vibrational distribution of fundamental and excited states. This is also confirmed by Matsumoto, Nakamura, and Eguchi,[30] who measured the electron temperature T_e by the double-probe technique in N_2 and N_2-H_2 (20% in N_2) plasmas and they did not observe significant differences in T_e between the two plasmas.

The analysis of the OES data, aimed to the evaluation of the N atom density in the plasma afterglow region, requires to establish the origin of the emitting species. It has been demonstrated[31-33] that in the afterglow region, where the electrons are absent or relaxed, the excitation of the $N_2(C^3\Pi_u)$ state is mainly given by the pooling reaction [see reaction (3) below] involving the $N_2(A^3\Sigma^+{}_u)$ metastable state that is reported to have a very long radiative lifetime of 1.9 sec,

$$N_2(A^3\Sigma^+{}_u) + N_2(A^3\Sigma^+{}_u) \rightarrow N_2(C^3\Pi_u) + N_2(X^1\Sigma^+{}_g). \tag{3}$$
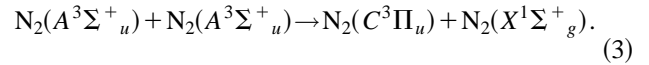
Thus, the emission intensity of the second positive system is representative of the $N_2(A^3\Sigma^+{}_u)$ density, which does not change by the H_2 and/or NH_3 addition.

As for the $N_2(B^3\Pi_g)$ state, it has been reported[34,35] that its formation in the afterglow, in absence of electrons, can occur by the following reactions: (a) the N atoms three-body recombination:

$$N + N + N_2 \rightarrow N_2(B^3\Pi_g) + N_2, \tag{4}$$
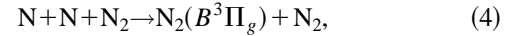
(b) the pooling reaction of $N_2(A^3\Sigma^+{}_u)$ metastables:

$$N_2(A^3\Sigma^+{}_u) + N_2(A^3\Sigma^+{}_u) \rightarrow N_2(B^3\Pi_g) + N_2(X^1\Sigma^+{}_g), \tag{5}$$
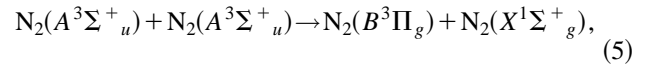
(c) the energy transfer of $N_2(A^3\Sigma^+{}_u)$ to $N_2(X^1\Sigma^+{}_g)$ molecules:

$$N_2(A^3\Sigma^+{}_u) + N_2(X^1\Sigma^+{}_g) \rightarrow N_2(B^3\Pi_g) + N_2(X^1\Sigma^+{}_g), \tag{6}$$
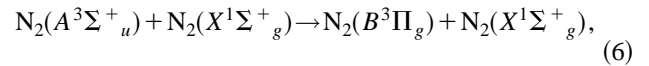
and (d) the radiative decay from the C state [see Eq. (2)].

On the basis of our experimental data presented above [in particular spectrum (c) of Fig. 1], the contribution of processes of Eqs. (2), (6), and (7) to the first positive system can be considered constant and very small. Consequently, the observed variation of the first positive system emission with H_2 and/or NH_3 addition (see Figs. 1 and 2) must be assigned to the N atom three-body recombination [Eq. (4)], which remains the main formation channel of the first positive system. Thus, the steady-state density of the $N_2(B^3\Pi_g)$ is representative of the N-atom density and, hence, the square-root emission intensity can be used as a measure of the N-atoms density[34]

$$I_{\text{first positive system}} \propto [N_2(B^3\Pi_g)] \propto [N]^2, \tag{7}$$

that is, the higher the intensity of the first positive system, the higher the N-atom density.

The decrease of N-atoms density observed when hydrogen is added to the N_2 plasma can be explained by the following scavenging process:[36]

$$x/2H_2(\text{or } xH) + N + M \rightarrow NH_x + M \quad (x = 1-3), \tag{8}$$

which gives NH_x ($x = 1-3$) species. The presence of the stable product NH_3 has been detected by MS sampling. In fact, Fig. 3 shows the variation of the signal at 17 amu due to the molecular ion $NH_3{}^+$ as a function of the H_2 percentage added to the N_2 plasmas. It is seen that the higher the hydrogen dilution, the higher is the concentration of the NH_3 produced. In addition, the inset of Fig. 3 shows that the MS signal of the $NH_3{}^+$ ion depends linearly on the N-atoms density (represented by the square root of the N_2 first positive-system emission intensity).

B. XPS analysis of GaN films

Figure 4 shows the XPS spectra of N $1s$, Ga $3d$, and As $3d$ photoelectron peaks for typical GaN layers obtained by N_2 and N_2-H_2 plasma nitridation of GaAs surfaces. For GaN layers prepared using N_2-NH_3 mixtures, the XPS spectra are
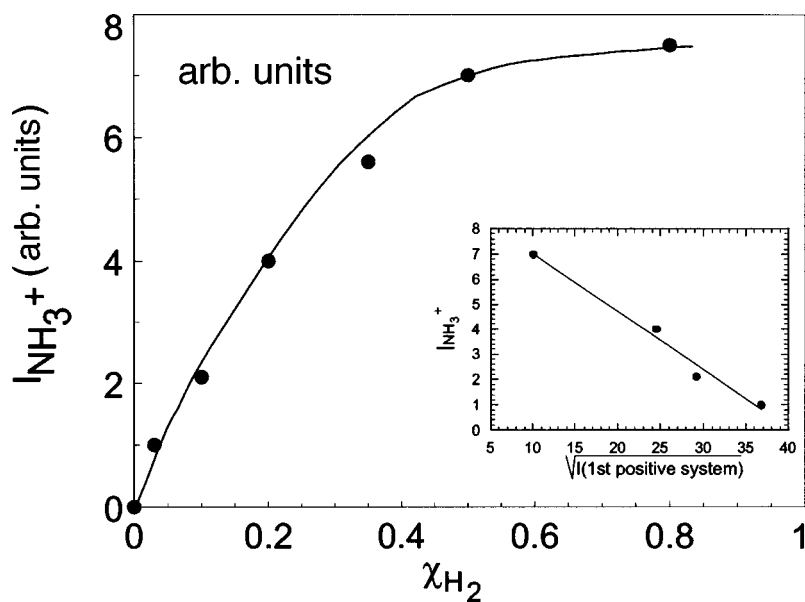
FIG. 3. Mass spectroscopic intensity of the molecular ion NH_3^+ at 17 amu vs the H_2 molar fraction in N_2 plasmas. The inset shows the linear correlation between the NH_3 formation and the N atoms density, which is represented by the square root of the emission intensity of the first positive N_2 system (see text).

nearly identical to those from the N_2-H_2 system. By using the relative atomic sensitivity factors of Ga $3d$ and N $1s$, the N/Ga concentration ratio has been calculated and reported in Fig. 4.

The Ga $3d$ peak for all the samples examined shows a main component assigned to GaN ($BE = 19.5$ eV).[37] Additional fitting components at $BE = 18.6$ eV due to metallic Ga and its oxidized form Ga_2O_3 at $BE = 20.4$ eV, are present in the GaN layers formed by N_2-H_2 and N_2-NH_3 plasma nitridations, so explaining the N/Ga$<$1. These Ga and Ga_2O_3 components are absent in the XPS spectra recorded for N_2 plasma nitridation samples, where the GaAs substrate component is present due to the small GaN thickness ($<$40 Å).

Nitridation by N_2 plasmas gives almost stoichiometric GaN layers. However, the broad As $3d$ peak indicates that As may exist in two different chemical states: the anions bonded with Ga and free As atoms resulting from the exchange reaction between N atoms and GaAs (see below). Angle-resolved XPS measurements provide evidence that the free As accumulates at the GaN/GaAs interface. The complete disappearance of the As signal in the thick GaN layers ($>$100 Å) formed by N_2-H_2 and N_2-NH_3 plasma indicates that the formed nitride layer is pure GaN, rather than the ternary compound $Ga_xAs_{1-x}N$, as reported by some authors.[6,14]

For all the experiments, the N $1s$ peak displays a shoulder at higher energy that is not due to As-N species as deduced from the As $3d$ spectra and probably is attributed to N-H or N-N bonds.

C. *In situ* real-time ellipsometric results

Figure 5 shows the $\langle \varepsilon_2 \rangle$ trends with evolution of the nitridation of GaAs recorded during typical nitridations of GaAs surfaces using N_2, N_2-H_2, and N_2-NH_3 rf plasmas and of a typical N_2-NH_3 thermal nitridation at a surface temperature of 700 °C, which is well above the thermal decomposition threshold of about 550 °C for the GaAs substrate. The observed different shapes of the $\langle \varepsilon_2 \rangle$ vs time data indicate that the replacement of As atoms with N atoms occurs via
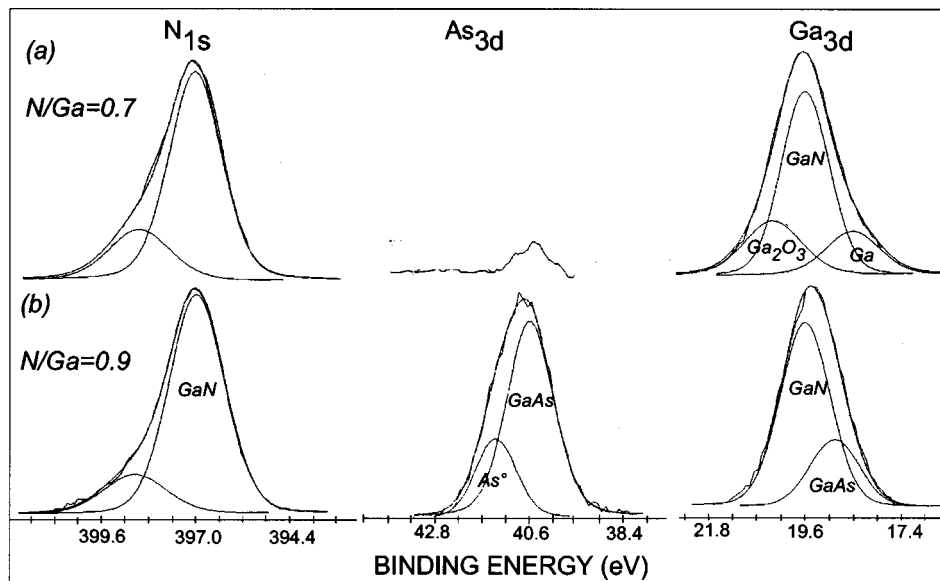
FIG. 4. Typical XPS spectra of the N $1s$, As $3d$, and Ga $3d$ photoelectron peaks for GaN layers obtained by (a) N_2-H_2 and N_2-NH_3 and (b) N_2 plasma nitridation of GaAs substrates. The corresponding N/Ga atomic ratio is also shown.
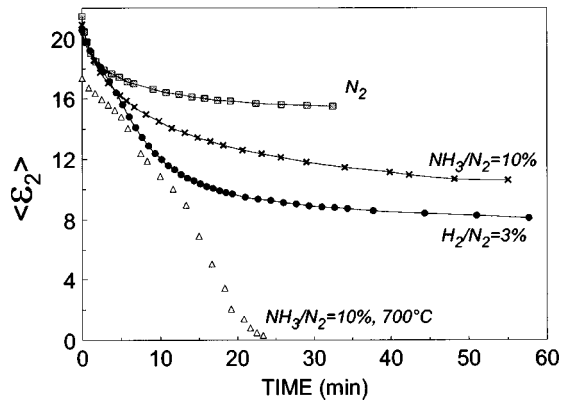
FIG. 5. $\langle \varepsilon_2 \rangle$ value at the photon energy of 4.5 eV vs time recorded during GaAs nitridation by (a) N_2 plasma at $T = 250$ °C, (b) N_2-H_2 (3% in H_2) plasma at $T = 250$ °C, (c) N_2-NH_3 (10% in NH_3) plasma at $T = 250$ °C, and (d) thermal nitridation by a N_2-NH_3 (10% in NH_3) mixture at $T = 700$ °C and $P = 1$ Torr. (Other plasma conditions: rf power = 200 W, $P = 0.2$ Torr.)

different kinetics. For the interpretation of these data and $\langle \varepsilon_2 \rangle$ spectra, it should be remembered that the pseudodielectric function is a composite function of both the chemistry and physics of the situation. In our case the pseudodielectric function is determined by not only the different chemistry, i.e., the composition of the GaN layers but also the crystalline structure, i.e., cubic or hexagonal GaN, the morphology, i.e., surface roughness and material microporosity. In order to discriminate among these effects, SE spectra have been acquired at the end of each of the nitridations and representative spectra in terms of $\langle \varepsilon_2 \rangle$ are shown in Fig. 6. These SE

spectra have been analyzed using BEMA models that are based on the XPS results and the models are depicted in Fig. 7, which also includes the values of the unbiased estimator χ^2 for the proposed models for the three plasma systems. The lowest χ^2 value indicates the best-fit model for each plasma nitridation system used in this study. The composition and thickness determined from the best-fit BEMA models for the SE spectra shown in Fig. 6, and that agree qualitatively with XPS results, are included with the best-fit model at the bottom of Fig. 6. Here, it is important to underline that the GaN pseudodielectric function $\langle \varepsilon \rangle$ used in the BEMA models is that of the hexagonal phase from Eduards, et al.[25] This choice does not mean that the present GaN layers are hexagonal, as we do not have any structure measurements. Since the uncertainty on the crystallinity of the present GaN layers, the SE data have been fitted by using the $\langle \varepsilon \rangle$ of either cubic and hexagonal phases. However, the comparison of the data derived by the two different fits does not show significant differences in layer thickness and composition. As an example, the SE spectrum (b) of Fig. 6 can be fitted by a single layer of $53 \pm 1\%$ α-GaN, $7 \pm 1\%$ Ga, and $40 \pm 1\%$ voids with a thickness of 100 ± 1 Å when hexagonal GaN is used, and alternatively, by a single layer of 52 $\pm 3\%$ β-GaN, $5 \pm 1\%$ Ga, and $43 \pm 2\%$ voids with a thickness of 100 ± 2 Å, when cubic GaN is included. Thus, the uncertainty, related to the use of α- or β-GaN, on the layer thickness and composition is in the range of the fitting error.

This insensitivity of the SE fitting to the GaN crystalline phase is a consequence of the nonideal crystallinity (grain-boundary regions, microporosity, surface roughness) of the GaN layers. However, the validity of the thickness values
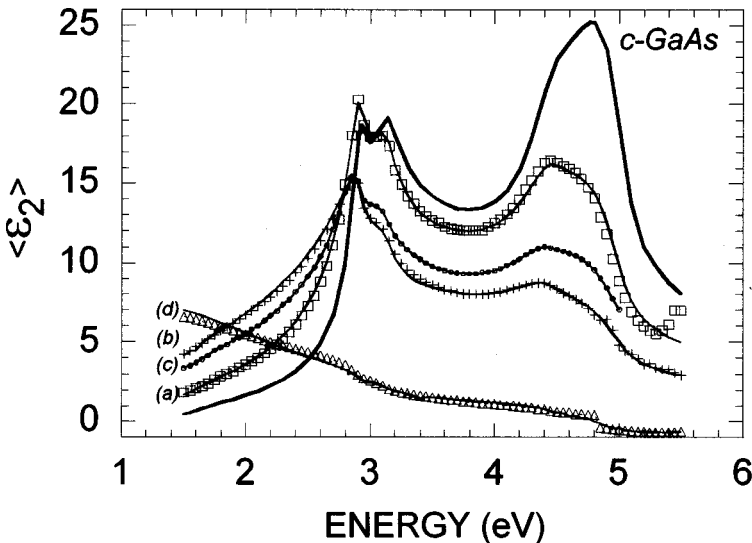
FIG. 6. SE spectra of the imaginary part of the pseudodielectric function $\langle \varepsilon_2 \rangle$ recorded at the end of the nitridation runs. Points are for experimental data and lines are for fit results. The corresponding best-fit BEMA models and χ^2 values are also shown.

54±2% GaN 46±1% void	40±1Å			55±1% GaN 37±1% void 8±1% Ga	60±1Å	18±1% GaN 80±1% void 2±1% Ga	288±5Å
53±1% GaN 40±1% void 7±1% Ga	100±1Å						
63±1% GaAs 37±2% a-As	7±1Å			15±1% GaN 85±1% GaAs	85±1Å	25±2% GaAs 11±1% Ga 64±1%void	325±5Å
c-GaAs		c-GaAs		c-GaAs		c-GaAs	

(a): N_2
$\chi^2 = 0.04$

(b): $H_2/N_2=3\%$
$\chi^2 = 0.02$

(c):$NH_3/N_2=50\%$
$\chi^2 = 0.03$

(d):$NH_3/N_2=10\%$, 700°C
$\chi^2 = 0.03$

FIG. 7. BEMA models used to fit the SE spectra. Plotted at the top is the unbiased estimator of the mean-square deviation for the solution to the model depicted at the bottom. The lines were drawn purely to indicate the χ^2 values for the same plasma system and to guide the eye.

FIG. 8. Time dependence of the GaN thickness obtained by nitridation with N_2-NH_3 plasmas at various NH_3 percentage. The GaN thickness profile by the N_2 plasma is also shown for comparison. Solid lines represent fit of the profiles by Eq. (19) defined in the text. (Other experimental conditions: $T = 250$ °C; rf power, 200 W; $P = 0.2$ Torr.)

derived from SE modeling has been confirmed by cross-sectional transmission electron microscopy (XTEM) measurements for a typical GaN layer nitrided by N_2/H_2 plasmas. The GaN thickness obtained from XTEM is about 12 nm, compared with 12.8 nm (53% GaN, 3% Ga, 44% voids) obtained from SE modeling.

As was mentioned above, the data in Figs. 5 and 6 suggest that a different surface chemistry is operative in each of the three plasma systems and in the following discussion we enumerate some key differences.

(1) For nitridation using pure N_2 plasmas, a two-layer model consisting of a lower-density GaN surface layer (GaN+voids) on a relatively higher-density interface layer composed of GaAs plus free As provides the best fit.

(2) For nitridation using N_2-H_2 and N_2-NH_3 plasmas with percentages of H_2 and/or NH_3 lower than 10%, the best-fit model is a single inhomogenous layer with three components (GaN+Ga+voids), which predicts the presence of metallic Ga in the nitrided layer.

(3) For nitridation using N_2-NH_3 plasmas with high NH_3 percentages, a two-layer model with an interface (GaN+GaAs) layer and a rough GaN surface layer containing free Ga and voids is best.

However, the models shown in Fig. 7 are applicable for nitridations performed at temperatures lower than the thermal decomposition threshold of the GaAs substrate ($T \leqslant 550$ °C). Nitridations done at $T > 550$ °C show a high-volume fraction of free Ga, which is even larger in the presence of H atoms. As an example, the GaAs nitrided at 700 °C are best fit by a two-layer model, in which the top layer is a rough mixture of GaN and Ga, and the interface layer is composed of damaged GaAs and Ga (see Fig. 6). Thus, from these results, it is concluded that both the nitridation chemistry and kinetics are strongly affected by the surface temperature and by the presence of H atoms.

In order to clarify the role of the surface temperature and of the H atoms on the nitridation mechanism, GaAs surfaces
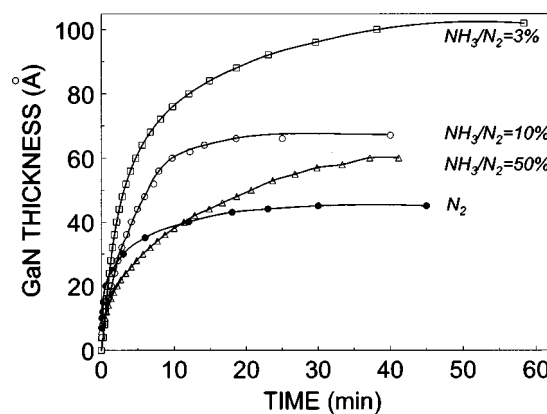
have been nitrided at various temperatures and at different gas-phase compositions and pressures. Each of the above best-fit BEMA models have been used to derive the corresponding GaN thickness profiles from the experimental $\langle \varepsilon \rangle$ profiles.

Figure 8 shows the time dependence of the GaN thickness during nitridation of the GaAs surface using N_2-NH_3 plasmas with various NH_3 percentages. Figure 9 shows the effect of H_2 addition on nitridation kinetics by N_2-H_2 plasmas for two different values of total pressure. In both figures the typical nitridation kinetics using a pure N_2 plasma is also reported for comparison. In all the three plasma systems, the GaN thickness vs nitridation time data is characterized by a relatively fast initial GaN formation followed by a progressive decrease of the nitridation rate and finally the achievement of a saturation GaN thickness. Typically, the saturation thickness, indicative of self-limiting growth, of 40 Å for the GaN layer has been observed using pure N_2 plasmas at T
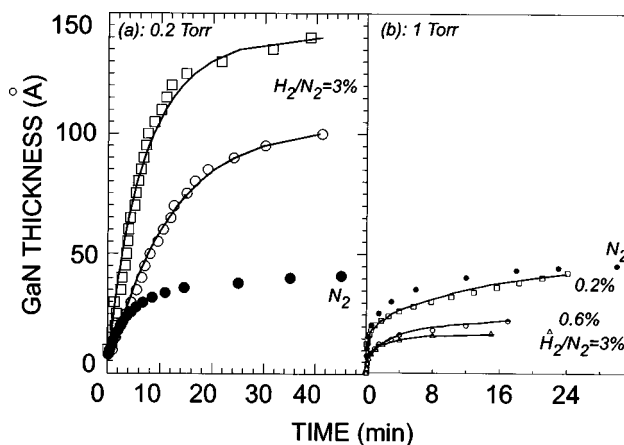
FIG. 9. Time dependence of the GaN thickness during nitridation by N_2-H_2 plasmas (a) at H_2/$N_2 = 3$%, $P = 0.2$ Torr and at (○) $T = 250$ °C and (□) $T = 350$ °C, and (b) at $T = 250$ °C, $P = 1$ Torr and different H_2 percentage. The GaN thickness profile by the N_2 plasma is also shown for comparison. Solid lines represent fit of the profiles by Eq. (21) defined in the text.
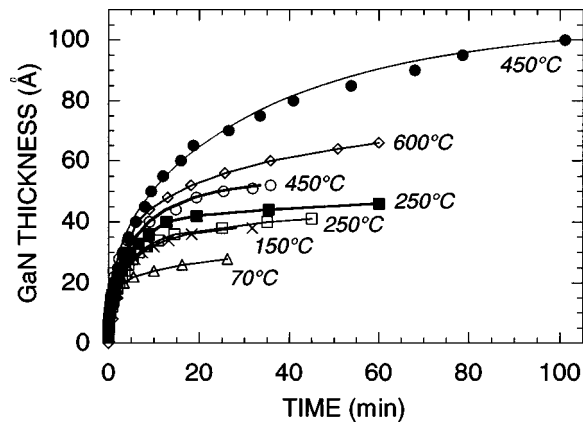
FIG. 10. GaN thickness profiles obtained by N_2 plasma nitridation at various temperatures at 0.2 Torr (empty symbols) and at 1 Torr (full symbols). Solid lines represent fit of the profiles by Eq. (21) defined in the text.

$=250\,°C$ for 1 h.[9,20] The presence of a few percent (3%) of hydrogen either as H_2 or NH_3 increases the GaN layers thickness, although the hydrogen addition decreases the N-atom density (see Figs. 1 and 2). However, the increase of the saturation GaN thickness by the H_2 or NH_3 addition is observed only at 0.2 Torr while at higher pressure (1 Torr) the H_2 addition effects a decrease of the GaN saturation thickness [see Fig. 9(b)]. In fact, at 1 Torr, the homogeneous recombination processes by hydrogen [Eq. (8)] and nitrogen [Eq. (4)] atoms become more effective than at 0.2 Torr, and the density of N atoms impinging on the surface is significantly reduced (OES data for N_2-H_2 experiments have shown a decrease of about 2–3 times in the relative density of N-atoms in going from 0.2 to 1 Torr). As expected, the lower N-atom density in N_2-H_2 plasmas at high pressure results in a smaller saturation thickness of GaN.

The effect of the GaAs surface temperature on the nitridation kinetics is reported in Fig. 10, which shows the GaN thickness profiles at various nitridation temperatures for N_2 plasmas. It is seen that the higher the temperature, the larger is the GaN thickness.[38] However, SE and AFM data[20] have shown that nitridation at $T>600\,°C$ yields GaN layers that are both very rough and Ga-rich, hence useless for most applications.

The temperature dependence of the nitridation kinetics for N_2-H_2 and N_2-NH_3 systems is more complex. For these cases, an upper limit of 450 °C is suggested for the nitridation. In fact, an almost flat $\langle \varepsilon_2 \rangle$ profile is found for $T=450\,°C$, indicating that nitridation of the GaAs surface does not occur. We believe this is due to the fact that for $T \geq 450\,°C$ the heterogeneous recombination of N atoms and H atoms, which desorb as NH_x species[39] dominates. In fact, above 450 °C, the XPS, SE, and AFM data have shown that only a small volume fraction of nitrogen is incorporated and that the GaAs surface rapidly deteriorates: the higher the temperature, the higher the damage in terms of roughness and Ga-enrichment of the GaAs surface.

D. Chemistry and kinetics

Differently from GaAs oxidation, where it has been possible to develop satisfactory chemical and kinetics models,[40,41] the GaAs nitridation cannot refer to any theoretical treatment.

The overall chemistry of the GaAs nitridation can be simply envisaged as

$$GaAs + N \rightarrow GaN + As. \qquad (9)$$
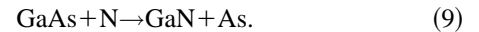
Limited by the inherent complications of this solid-state exchange reaction, we only consider the overall reaction characteristics and analyze the kinetics on the basis of the canonical laws of the gas-solid interactions.

Thus, Eq. (9) is analyzed in the framework of the heterogeneous reactions in which the following steps are considered: (i) chemisorption of nitriding species, N atoms and/or NH_x radicals, at the beginning on the GaAs surface and afterwards on the GaN surface; (ii) inward migration of N atoms through the product GaN layer, and toward the GaN/GaAs interface, which at first can be considered to occur via Fickian diffusion; (iii) chemical reactions at the GaN/GaAs surface, involving the N atoms chemisorption and the exchange reaction of As with N, the formation of AsN and, when in the presence of H atoms, of AsH_x species; (iv) desorption and outward migration of the As products, also via Fickian diffusion.

We excluded the outward migration of Ga and As ions based on their high mass compared to N atoms, the large ionic sizes, and also because voltage bias assisted nitridation does not show any effect even under favorable conditions unlike GaAs oxidation.[28]

The problem of establishing which of the above steps controls the nitridation rate and depth is difficult. While the concentration of nitrogen atoms (and/or NH_x radicals) in the gas phase depends on electron impact dissociation processes and on recombination processes (especially the latter in the downstream plasma region), the amount of nitrogen at the GaN/GaAs interface, obviously depends on step (ii), which is the N supply function. In order to determine whether transport controls the overall nitridation process, we prepared thickness vs the square root of time and found that the plots are not linear, which indicates that the overall nitridation process is not determined by the N atom in diffusion. In fact, we can exclude both Fickian transport (chemical diffusion) and also flow-in micropores (Knudsen-Poiseuville flow) where both transport processes yield parabolic kinetics in which the N-atoms transport is simply inversely proportional to the GaN thickness oxidation.[42] While this may appear counter intuitive, the typical examples of diffusion controlled reactions for apparently similar cases include Si nitridation[43] and Si oxidation,[42] where in both cases the molar volume of the solid product (Si_3N_4 or SiO_2) is larger than that of the reactant (Si). The consequence is a compressive film stress and the products Si_3N_4 or SiO_2 form a protective layer or diffusion barrier on Si with the result that the overall reaction rate is controlled by the low diffusivity of nitrogen or oxygen through the Si_3N_4 or SiO_2 barrier layer. The situation for GaAs nitridation is essentially the opposite where the molar volume of the solid product (GaN) is less than that of the reactant (GaAs). In this case, the product layer (GaN) could be microporous (this is supported by our SE modeling results, which require GaN+voids to achieve the best fit), resulting in rapid transport so that the rate-determining step may be the chemical process occurring at the GaN/GaAs interface. Under these circumstances the rate is determined by the available surface area of GaAs, and such a process is

referred to as ''*topochemical.*'' [44] Topochemical reactions are greatly affected by any substance different from the nitriding species that adsorbes on the reactant surface and thus reduces the area of the GaAs surface available for reaction. Such an interfering substance behaves as an *inhibitor* or *poison*. In the particular case of GaAs nitridation, the reaction product As appears at the GaAs surface as was evidenced in the SE models, which show As segregation. The As could inhibit the reaction and at the same time modify the kinetic law. Based on these assertions, a simple chemical model for the GaAs nitridation is as follows:

$$
\begin{array}{c}
\overset{D}{N} \rightarrow N(bulk) + GaAs \overset{k}{\rightarrow} GaN + As \\
+ \\
As \\
k_r \downarrow \\
AsN \rightarrow 1/2 N_2 + As
\end{array}
$$
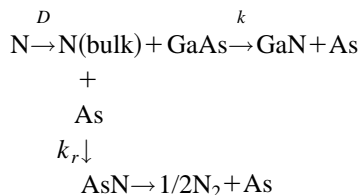
where D is the diffusion coefficient for the in diffusion of N atoms, k is the true rate constant of the reactive step at the GaAs surface yielding GaN and free As, and k_r is the rate constant for the N-atoms recombination reaction also activated by the As sites. The existence of AsN species at temperatures lower than 250 °C has been reported by Masuda *et al.*[6] The fate of As depends on the plasma system. During nitridation by pure N_2 plasmas, As atoms segregate at the GaN/GaAs interface, thus reducing both the N-atom density and the GaAs exposed surface. For nitridation by N_2-H_2 and N_2-NH_3 plasmas, the presence in the bulk of H atoms facilitates the formation of AsH_x species, which outdiffuse and reduces the As segregation. However, the chemical nitridation model above is valid at $T < 550$ °C, since at surface temperatures higher than 550 °C, the nitridation is assisted by the GaAs thermal decomposition, whatever is the plasma system.[20]

Using the chemical model, a rate law for GaAs plasma nitridation is derived and tested against the measured thickness time data. To this end we start from the steady-state conditions applied to the N atoms flux F. In the kinetic model we consider the following fluxes (see scheme in Fig. 11).

First is the Fickian flux F_1 for the indiffusion of N atoms:

$$
F_1 = -D \frac{\partial c}{\partial x} = \frac{D(c_0 - c_N)}{x}, \tag{10}
$$

where D is the diffusion constant of the N atoms through the GaN layer of thickness x, and c_0 and c_N are the N-atom density at the outermost surface and at the GaN/GaAs interface, respectively. While we have assumed Fickian diffusion of N atoms, it is important to realize that an alternative transport mode is flow-through micropores, but Knudsen-Poiseuville flow has a similar inverse thickness dependence and as such the two flux equations are virtually indistinguishable.[42] Next is the flux of N atoms F_2 involved in the heterogeneous recombination to yield N_2 and/or AsN:
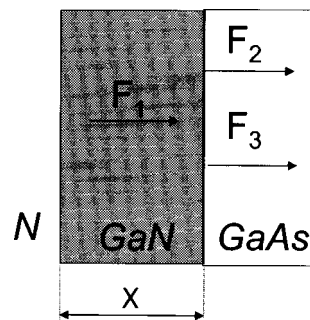
FIG. 11. Schematic representation of the steady-state N-atom fluxes ($F_1 = F_2 + F_3$) involved in the GaAs nitridation to GaN. F_1 is the diffusive/transport flux of N atoms to GaN/GaAs interface; F_2 is the recombination flux to AsN/N_2 and F_3 is the reaction flux to GaN.

$$
F_2 = k_r c_N, \tag{11}
$$

where k_r is the recombination rate constant, whose value will depend on the presence/absence of free As (see the chemical scheme above). Finally, there is the flux F_3 of N atoms involved in the reaction, at the GaN/GaAs interface, yielding GaN:

$$
F_3 = k c_N S_{GaAs} \propto k c_N \left(1 - \frac{x}{a} \right) = \frac{k}{a} c_N (a - x), \tag{12}
$$

where k is the true rate constant for the surface reaction step and S_{GaAs} is the area of the exposed GaAs surface (*topochemical reaction*), also related to the number density of surface-active sites. In the present case, the area of the exposed GaAs surface does not remain constant during the nitridation process. In fact, S_{GaAs} decreases while nitridation is operative, because of the segregation of free As at the GaN/GaAs interface, which reduces the number of GaAs sites for nitridation. Thus, the S_{GaAs} decrease can be simply related to GaN thickness by the term $(1 - x/a)$, where a is the saturation GaN thickness. Now assuming a steady state where the following relation obtains:

$$
F_1 = F_2 + F_3 \tag{13}
$$

and

$$
\frac{D(c_0 - c_N)}{x} = k_r c_N + \frac{k}{a} c_N (a - x). \tag{14}
$$

The solution for N-atom density is given as

$$
c_N = \frac{D c_0}{D + k_r x + \frac{k}{a}(a - x)x}. \tag{15}
$$

This equation enables the flux F_3 to be expressed as

$$
F_3 = \frac{\partial x}{\partial t} = \frac{k}{a}(a - x) \frac{D c_0}{D + k_r x + \frac{k}{a}(a - x)x}. \tag{16}
$$

The relationship between GaN thickness x and time t is obtained by integrating Eq. (16) and yields the following equation for the time evolution of the nitridation:

TABLE I. Values of the best-fit parameters by (a) Eq. (19) and (b) Eq. (22) (see text) for the experimental GaN thickness profiles obtained by the three plasma systems.

	N$_2$				N$_2$-NH$_3$ ($T=250$ °C)			N$_2$-H$_2$ (3% in H$_2$)	
	70 °C	150 °C	250 °C	450 °C	3% NH$_3$	10% NH$_3$	50% NH$_3$	250 °C	350 °C
					(a)				
A	7.56	8.76	13.40	15.50	15.35	14.21	14.46	7.18	9.22
B	0.50	0.29	0.38	0.34	0.14	0.17	0.24	0.0005	0.018
C	0.013	0.003	0.0019	0.0011	0.000 08	0.002	0.004	0.0005	0.000 08
a	29	39	41	54	103	70	65	101	141
					(b)				
a	28	39	41	54	103	70	65	103	141
b	1.04	1.33	1.15	1.57	0.12	0.021	0.008	0.0006	0.0042
k'	4.51	5.09	5.50	6.02	0.86	0.33	0.27	0.087	0.177

$$t = \frac{a(D+ak_r)}{kDc_0} \ln \frac{a}{a-x} - \frac{k_r a}{kDc_0} x + \frac{1}{2Dc_0} x^2, \quad (17)$$

which can be rewritten for ease of manipulation as

$$t = A \ln \frac{a}{a-x} - Bx + Cx^2. \quad (18)$$

This equation has been used to fit all the experimental $x(t)$ profiles; the best fit A,B,C parameters have been derived and are listed in Table I(a). Interestingly, we found that for all experiments the $C(=1/2Dc_0)$ values are almost equal to zero ($<10^{-2}$) and, therefore, negligible with respect to other terms. We conclude that the transport term whether by diffusion or micropore flow is fast, and therefore kinetically not important. Thus, Eq. (18) reduces to

$$t = A \ln \frac{a}{a-x} - Bx, \quad (19)$$

or in its complete form [see Eq. (17)],

$$\frac{kc_0}{a} t = \frac{D+ak_r}{D} \ln \frac{a}{a-x} - \frac{k_r}{D} x. \quad (20)$$

This equation reduces to the following:

$$k't = (1+ab)\ln \frac{a}{a-x} - bx \quad (21)$$

and includes, as a fitting parameters, the constants k' and b, which are representative of the true-rate constant k of the surface-reactive step, and of the disappearance of N atoms through the As-activated recombination k_r. The fitting of all the experimental $x(t)$ profile (Figs. 8–10) by Eq. (21) produce the values listed in Table I(b). The parameter a represents the maximum nitridation depth. The b parameter is a measure of the reaction inhibition by the As poison, and its value increases with temperature (in fact an increase of As segregation at the GaN/GaAs interface has been found[20]) and decreases with H$_2$ and/or NH$_3$ addition. The presence of hydrogen favors the As desorption, and the higher the H atom content, the lower the b value. The pseudorate constant k' obviously increases with temperature and its value depends on the plasma mixture, being higher for pure N$_2$ plasmas

than for N$_2$-NH$_3$ and N$_2$-H$_2$ plasmas. The fact that the k' value decreases when in the presence of hydrogen is because it includes besides the k constant, the N atoms density c_0, which decreases with the H$_2$ and NH$_3$ addition (see Figs. 1 and 2) and the saturation thickness a, which is lower for N$_2$ plasmas than for N$_2$-NH$_3$ and N$_2$-H$_2$ plasmas.

The temperature variation of the pseudorate constant k' can be examined using an Arrhenius plot to derive the apparent activation energy E'_a of the nitridation process. The low value of E'_a of 0.05 eV can be understood using the fact that for gas-solid reactions the true activation energy E_a is reduced by the heat of adsorption of the reactant (N atoms).

Also, a direct consequence of the suggested nitridation model is that, with other parameters kept constant, the amount of nitrogen incorporated as the GaN layer depends upon the partial pressure of N atoms in the gas phase. In particular, the initial nitridation rate, i.e., the rate at the very beginning of the nitridation process, is a measure of the N-atom density at the gas-solid interface. Equation (16) evaluated for $x=0$ reduces to

$$\left(\frac{dx}{dt} \right)_{x=0} = kc_0, \quad (22)$$

whose validity is confirmed by the data shown in Fig. 12,
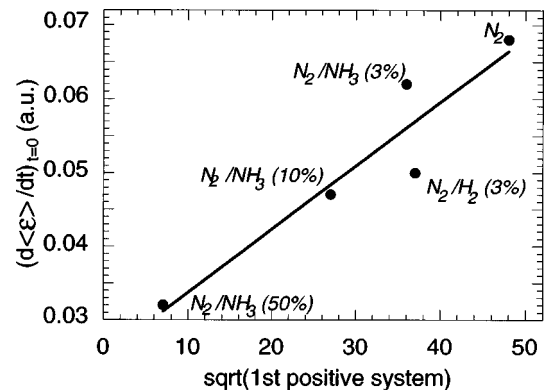
FIG. 12. Linear correlation between the initial nitridation rate, in terms of $d\varepsilon/dt$, and N-atom density evaluated by the square root of the first N$_2$ emission system.

where the initial nitridation rate, in terms of $d\varepsilon/dt$, is plotted as a function of the N-atom density, in terms of the square root of the first N_2 emission system (see Sec. III A).

IV. CONCLUSIONS

The GaAs nitridation by N_2, N_2-H_2, and N_2-NH_3 remote plasmas has been investigated *in situ* and in real time using spectroscopic ellipsometry, and the following conclusions are drawn.

The GaAs nitridation is a *topochemical* reaction, i.e., the nitridation rate is determined by the area of the GaAs surface available for the N-atoms chemisorption.

Free As has a dual inhibiting role in the nitridation kinetics: it is a recombination site of N atoms by forming AsN and, since it segregates at the GaN/GaAs interface, As reduces the available GaAs surface.

The GaAs nitridation is a self-limiting process and is inhibited by As, which segregates at the GaN/GaAs interface and limits the thickness of the GaN layers formed by N_2 plasmas to few tens of angstroms. In N_2-H_2 and N_2-NH_3 plasmas, the presence of a small amount of H atoms ($\sim 3\%$) promotes the As desorption as AsH_x, so reducing the poisoning effect of As and increasing the GaN thickness (>100 Å).

A very narrow range of surface temperature exists where the GaAs plasma nitridation can be operated successfully. In N_2 plasmas, at $T>600\,°C$ GaAs surface decomposes yielding very rough and Ga-rich GaN layers. In N_2-H_2 and N_2-NH_3 plasmas, the nitridation does not occur when $T \geq 450\,°C$ because of the heterogeneous recombination process of N and H atoms.

The composition and morphology of the GaN layers depends on the plasma mixture. N_2 plasmas yield stoichiometric and smooth GaN layers with As segregation at the GaN/GaAs interface. N_2-H_2 and N_2-NH_3 plasmas give Ga-rich GaN layers without As segregation. However, the excess Ga can be easily nitrided by a subsequent exposure for few min to a N_2 plasma.

Nitridation using N_2-H_2 plasmas yield very stable GaN layers, since neither etching nor damage is induced by submitting the GaN layers to H atom plasma treatments, even at temperature as high as $500\,°C$ and at very high H atom doses. On the contrary, GaN layers prepared using either N_2 or N_2-NH_3 plasma nitridation are easily etched by H atoms treatments.[45]

*Author to whom correspondence should be addressed. FAX: +39.80.5442024. Electronic address: cscpgb02@area.ba.cnr.it

[1] S. Nakamura, T. Mukai, and M. Senoh, Appl. Phys. Lett. **64**, 1687 (1994).

[2] S. Nakamura, M. Senoh, N. Iwasa, and S. Nagahama, Appl. Phys. Lett. **67**, 1868 (1995).

[3] S. Nakamura, MRS Bull. **17**, 29 (1997).

[4] S. J. Pearton and C. Kuo, MRS Bull. **17**, 29 (1997).

[5] Q. J. Xu, X. M. Ding, X. Y. Hou, and X. Wang, Appl. Surf. Sci. **104/105**, 468 (1996).

[6] A. Masuda, Y. Yonezawa, A. Morimoto, and T. Shimizu, Jpn. J. Appl. Phys., Part 1 **34**, 1075 (1995).

[7] L. A. DeLouise, J. Vac. Sci. Technol. A **10**, 1637 (1992).

[8] K. W. Vogt and P. A. Kohl, J. Appl. Phys. **74**, 6448 (1993).

[9] P. Hill, D. I. Westwood, L. Haworth, J. Lu, and J. E. Macdonald, J. Vac. Sci. Technol. B **15**, 1133 (1997).

[10] S. Fujieda and Y. Matsumoto, Jpn. J. Appl. Phys., Part 2 **30**, L1665 (1991).

[11] A. Kikuchi, H. Hoshi, and K. Kishino, Jpn. J. Appl. Phys., Part 1 **33**, 688 (1994).

[12] R. J. Hauenstein, D. A. Collins, X. P. Cai, M. L. O'Steen, and T. C. McGill, Appl. Phys. Lett. **66**, 2861 (1995).

[13] O. Brandt, H. Yang, A. Trampert, M. Wassermeier, and K. H. Ploog, Appl. Phys. Lett. **71**, 473 (1997).

[14] M. E. Jones, J. R. Shealy, and J. R. Engstrom, Appl. Phys. Lett. **67**, 542 (1995).

[15] N. Kuwano, Y. Nagatomo, K. Kobayashi, K. Oki, S. Miyoshi, H. Yaguchi, K. Onabe, and Y. Shiraki, Jpn. J. Appl. Phys., Part 1 **33**, 18 (1994).

[16] T. S. Cheng, L. C. Jenkins, S. E. Hooper, C. T. Foxon, J. W. Orton, and D. E. Lacklison, Appl. Phys. Lett. **66**, 1509 (1995).

[17] O. Brandt, H. Yang, B. Jenichen, Y. Suzuki, L. Daweritz, and K. H. Ploog, Phys. Rev. B **52**, R2253 (1995).

[18] O. Brandt, H. Yang, and K. H. Ploog, Phys. Rev. B **54**, 4432 (1996).

[19] G. Bruno, M. Losurdo, and P. Capezzuto, J. Vac. Sci. Technol. A **13**, 349 (1995).

[20] M. Losurdo, P. Capezzuto, G. Bruno, P. R. Lefebvre, and E. A. Irene, J. Vac. Sci. Technol. B **16**, 2665 (1998).

[21] D. A. G. Bruggemann, Ann. Phys. (Leipzig) **24**, 636 (1935).

[22] D. E. Aspnes and A. A. Studna, Phys. Rev. B **27**, 985 (1983).

[23] G. N. Greaves, E. A. Davis, and J. Bordas, Philos. Mag. **34**, 265 (1976).

[24] J. Petalas, S. Logothetidis, S. Boultadakis, M. Alouani, and J. M. Willis, Phys. Rev. B **52**, 8082 (1995).

[25] N. V. Edwards, M. D. Bremser, T. W. Weeks, R. S. Kern, R. F. Davis, and D. E. Aspnes, Appl. Phys. Lett. **69**, 2065 (1996).

[26] The SE spectrum of hexagonal GaN has been measured by us on a sample (5-μm-thick on sapphire) supplied by EMCORE.

[27] G. Bruno, P. Capezzuto, and M. Losurdo, Phys. Rev. B **54**, 17 175 (1996).

[28] M. Losurdo, P. Capezzuto, and G. Bruno, Phys. Rev. B **56**, 10 621 (1997).

[29] R. W. B. Pearse and A. G. Gaydon, *The Identification of Molecular Spectra*, 4th ed. (Wiley, New York, 1976).

[30] S. Matsumoto, H. Nakamura, and S. Eguchi, in *Plasma Synthesis and Etching of Electronic Materials*, edited by R. P. H. Chang and B. Abeles, MRS Symposia Proceedings No. 38 (Materials Research Society, Pittsburgh, 1985), p. 461.

[31] S. De Benedictis and G. Dilecce, Chem. Phys. **192**, 149 (1995).

[32] J. L. Jaubertau, D. Conte, M. I. Baratou, P. Quintard, J. Aubreton, and A. Chaterinot, Plasma Chem. Plasma Process. **10**, 412 (1990).

[33] L. G. Piper, J. Chem. Phys. **88**, 231 (1988).

[34] J. Al Andari, A. M. Diamy, L. Hochard, J. C. Legrand, and A. Ricard, in *Proceedings of 13th International Symposia on Plasma Chemistry* (Beijing, China, 1997), edited by C. K. Wu (Peking University Press, Beijing, 1997), Vol. I, p. 373.

[35] L. G. Piper, J. Chem. Phys. **88**, 6911 (1988).

[36] J. Amorim, G. Baravian, and A. Ricard, Plasma Chem. Plasma Process. **15**, 721 (1995).

[37] J. F. Moulder, W. F. Stickle, P. E. Sobol, and K. D. Bomben, in *Handbook of X-ray Photoelectron Spectroscopy*, edited by J. Chastain (Perkin-Elmer, Eden Prairie MN, 1992).

[38] M. E. Jones, J. R. Shealy, and J. R. Engstrom, Appl. Phys. Lett.

67, 542 (1995).

[39] Y. M. Sun and J. G. Ekerdt, J. Vac. Sci. Technol. B **11**, 610 (1993).

[40] N. Cabrera and N. F. Mott, Rep. Prog. Phys. **12**, 163 (1948).

[41] K. Yamasaki and T. Sugano, J. Vac. Sci. Technol. **17**, 959 (1980).

[42] E. A. Irene, J. Appl. Phys. **54**, 5416 (1983).

[43] S. Wolf and R. N. Tauber, in *Silicon Processing for the VLSI Era* (Lattice, Sunset Beach, CA, 1986), Vol. I, p. 210.

[44] K. J. Laidler, *Chemical Kinetics* (McGraw-Hill, New York, 1965), p. 316.

[45] M. Losurdo, P. Capezzuto, and G. Bruno, Thin Solid Films **313–314**, 501 (1998).